Int J Adv Manuf Technol (2010) 50:163–174
DOI 10.1007/s00170-009-2506-9

ORIGINAL ARTICLE

A comparative study of material phase effects on micro-machinability of multiphase materials

Aamer J. Mian · Nicholas Driver · Paul T. Mativenga

Received: 9 July 2009 / Accepted: 22 December 2009 / Published online: 30 January 2010

Abstract In the mechanical micro-machining of multiphase materials, the cutting process is undertaken at a length scale where material heterogeneity has to be considered. This has led to increasing interest in optimising the process parameters for micro-machining of such materials. In this study the micro-machinability of two steels, a predominantly ferrite material (AISI 1005) and a near-balanced ferrite/pearlite microstructure (AISI 1045) was studied. Workpiece sample deformation properties were characterised by nano-indentation testing. Additionally, metallographic grain size evaluation was undertaken for the workpiece microstructures. Surface roughness, workpiece microstructure and burr size for micro-machined parts as well as tool wear were examined over a range of feed rates. The results suggest that for micro-machined parts, differential elastic recovery between phases leads to higher surface roughness when the surface quality of micro-machined multiphase phase material is compared to that of single phase material. On the other hand, for single phase predominantly ferritic materials, reducing burr size and tool wear are major challenges. Thus, the paper elucidates on material property effects on surface and workpiece edge quality during micro-milling.

Keywords Micro-milling · Microstructure effect · Size effect

1 Introduction

1.1 Micro-machining

Micro-mechanical machining offers great potential for manufacturing complex micro components [1–5]. The technology can be described as the process of removing material from a workpiece in the form of chips typically in the micron or sub-micron length scale. For some coarse grained material, this chip formation can take place at a length scale smaller or comparable to the individual grains of a material microstructure [6]. Simoneau et al. suggested that the cutting domain could be moved between macro-, meso- and micro-scale by altering grain sizes of the workpiece material [7]. Hence, some polycrystalline material must be treated as discrete and heterogeneous at this level [8]. Taking into account the challenges met in micro-machining, ultra fine grain, hard and high homogeneous workpiece materials are considered ideal for manufacturing micro components [1, 5, 9]. Thus, it becomes desirable to develop a deeper understanding of the fundamental mechanisms associated with the material microstructure behaviour under different cutting conditions.

The present study is a continuation of a previous work regarding multiphase material microstructure effect in micro-milling [10]. The already published paper focussed on the micro-milling of one coarse grained AISI 1045 steel workpiece material. This new paper extends the research work and reports on the micro-machinability of single compared to multiphase ferrous workpiece materials.

1.2 Material microstructure effect on surface generation in micro-machining

The ratio of surface area to volume increases as devices and their features are miniaturised. For this reason, in micro component manufacture, more attention should be given to surface generation and phenomena that affect the surface character. At micro-scale it was reported that the tool–workpiece material interaction strongly influences the machined surface topography [11]. Weule et al. reported by utilising different heat treated AISI 1045 steel that when micro-machining (fly cutting), variation in material property from one grain to the next influenced the resulting

A. J. Mian (✉) · N. Driver · P. T. Mativenga
Manufacturing and Laser Processing Group,
School of Mechanical, Aerospace and Civil Engineering,
The University of Manchester,
M60 1QD Manchester, UK
e-mail: Aamer.Mian@postgrad.manchester.ac.uk

surface finish [5]. It was suggested that surface roughness varies between the grains of material and is influenced by the tool edge radius, microstructure phases, minimum chip thickness effects [12], crystallographic orientation [13], material elastic recovery and phase dependent elastic-plastic anisotropy [9]. Furthermore, for single crystal face centred cubic (f.c.c.) materials, intrinsic plastic behaviour of individual crystals was reported to have more dominant effect on surface roughness compared to with crystallographic cutting direction [13]. Plastic strain mismatch, grain orientation relative to cutting edge and large energy absorption in harder phases cause surface defects on the multiphase microstructure of AISI 1045 steel [14, 15].

Son et al. reported the best surface finish which occurred at the minimum chip thickness for aluminium, brass and copper workpiece materials and observed that this was associated with the formation of continuous chips [16]. The dominant influence of chip thickness on surface roughness in micro-machining was reported in literature [5, 12, 17]. It was suggested that the effect of crystallographic orientation on surface roughness could be alleviated by selecting chip loads ten times larger than the grain size of the specific material [18]. Moreover, improvement in the surface integrity and quality of micro-machined parts can also be achieved through metallurgical and mechanical grain structure modifications [19]. However, this is not always desirable since modifying a material's microstructure changes its properties and can affect functional performance. This case is more critical if micro features are on a large component.

1.3 Burrs in micro-machining

Burr formation is a critical factor in micro-machining since it affects the capability to meet desirable tolerance and geometry definition [4, 5, 20]. Gillespie highlighted that minimisation of burr size is most desirable as conventional de-burring process could cause dimensional imperfections and residual stresses in miniature precision parts. Moreover, post-processing for burr removal could often constitute 30% of the cost to produce a part [21]. There are three generally accepted burr formation mechanisms namely; lateral deformation, chip bending and chip tearing. Four basic types of burrs were defined as Poisson, tear, rollover and cut-off burrs [22]. The formation of burrs progresses through stages of initiation, initial development, pivoting point and final development [23].

In terms of burr control, Nakayama and Arai [24] proposed that in macro-scale machining, the size of the sideward burr could be minimised by decreasing the undeformed chip thickness and reducing shear strain of the chip. It is noted here that in micro-machining, decreasing chip thickness only helps reduce burr size when machining at undeformed chip thickness greater than the tool edge radius. Otherwise ploughing effects would promote relatively larger burr size. Turning the direction of cutting force towards the workpiece and strengthening the workpiece edge was proposed to be useful in this regard [24]. Material properties also influence burr formation. In general, it was suggested that the workpiece materials with a higher ductility produce larger burr size [25].

Burr formation is driven by the size effect, with a larger tool edge radius leading to larger burrs [25–27]. Cutting modes in slot milling also generates different burr size. Filiz et al. reported larger size of burr in down milling as compared to up milling [26]. Fang and Liu suggested that once the workpiece material and other process parameters are specified, the undeformed chip thickness will determine burr height [28]. The enlargement in the tool edge radius which occurs due to tool wear decreases the ratio of undeformed chip thickness to cutting edge radius; this means that effective rake angle becomes more negative. Material ahead of the tool is pushed/compressed and deformed plastically into a burr.

1.4 Research motivation

From the reviewed literature, it is clear that the machinability of micro parts would be favourable if all parts were made from single phase materials with a very fine microstructure and preferably low ductility. However, in practice, micro components are manufactured from typical engineering materials that contain multiphase structures.

In building a scientific base for machining such materials, it was decided to select two binary phase materials one dominated by a single phase and the other with an almost balanced volume fraction. Studying the machinability of these materials would enable the elucidation of the effect of phase properties on surface roughness and subsurface microstructure change in the micro-machining process.

2 Experimental details and evaluations

2.1 Material metallographic grain size measurement

The selected workpiece materials were AISI 1005 and 1045 steel alloy. AISI 1005 steel is 99% ferrite content while 1045 steel can be considered as representing balanced volume fractions of ferrite and pearlite. The microstructure of these materials is shown in Fig. 1. The grain size of AISI 1005 steel was evaluated according to BS EN ISO643:2003 [29] and found to be on average 67 μm. For AISI 1045 steel, the grain size was determined by the linear intercept method. In Fig. 1, the white surface is the ferrite phase and

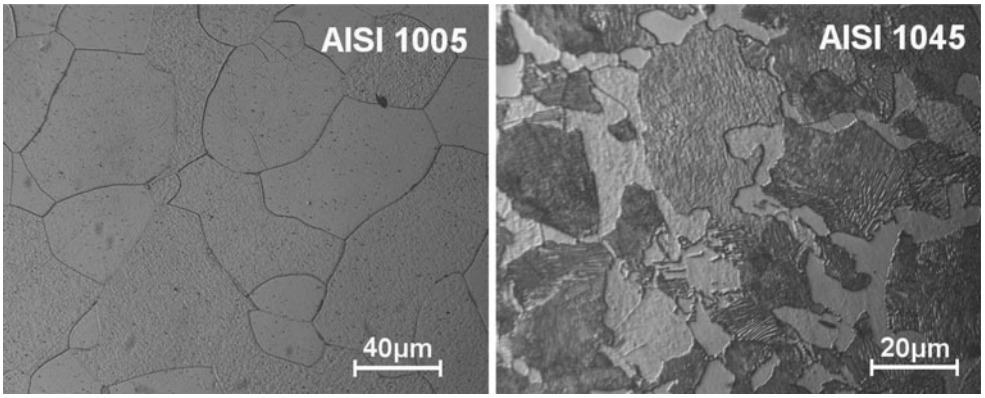

Fig. 1 Workpiece microstructure. **a** AISI 1005 steel. **b** AISI 1045 steel

its average grain intercept length was 7 μm. The black regions are the pearlite phase with 52-μm average grain intercept length.

2.2 Material characterisation using instrumented indentation testing

A model XP nanoindenter supplied by MTS instruments was used for material characterisation. Each test was performed ten times on three different samples of each workpiece material. Indentation depth was varied from 0.2 to 2 μm. A standard Berkovich indenter was used because it induces plasticity at very low loads. The load and indenter displacement were recorded simultaneously during the entire loading and unloading process. Hence, the process was capable of measuring both the plastic and elastic deformation of the materials under test [30]. Table 1 shows the average elastic modulus and nano-hardness data computed from the unloading data and their standard deviation. It is clear that the variability between measurements is very low. However, in comparing workpieces, there is low variability for a single phase material compared to the multi-phase AISI 1045 steel. This can be attributed to the different properties of ferrite and pearlite. The data shows that AISI 1045 steel is relatively harder than AISI 1005 steel. The hardness behaviour of a material is normally related to its resistance to plastic deformation. Therefore, it can be expected that AISI 1005 steel, being of lower hardness, will plastically deform more.

In scratch testing of polymers and metals, Jardret et al. [31] noted that the proportion of the plastic deformation increases with an increase of the Young's modulus to hardness ratio. Using this assumption, it can be inferred from Fig. 2a that AISI 1005 steel will plastically deform more compared to 1045 steel. On the other hand, Nakayama [32] attributed larger elastic recovery to a high ratio of the hardness to elastic modulus. In order to quantify the elastic recovery of the investigated materials, displacement into the surface was analysed. The percentage of elastic recovery was calculated by taking the difference between maximum indentation depth when fully loaded and residual indentation depth after unloading. The results are shown in Fig. 2b. It is evident from the graph that AISI 1045 steel has a higher elastic recovery compared to AISI 1005 steel. The elastic recovery decreases with a reduction in indentation depth. This validates the use of hardness to elastic modulus ratio in predicting elastic deformation. Thus, it is clear from the nano-indentation testing that pearlite and ferrite have differential deformation patterns and a ferrite structure is expected to show deeper plastic deformation.

Table 1 Mechanical properties variation as a function of nano-indentation depth

Nano-indentation depth (μm)	AISI 1005 steel				AISI 1045 steel			
	Nano-hardness		Elastic modulus		Nano-hardness		Elastic modulus	
	Average (GPa)	Standard deviation	Average (GPa)	Standard deviation	Average (GPa)	Standard deviation	Average (GPa)	Standard deviation
0.2	2.65	0.18	231.75	30.9	3.53	0.81	220.8	16.5
0.5	2.43	0.37	233.05	14.3	3.49	0.32	241.5	9.64
1	2.20	0.34	236.36	10.01	2.89	0.40	238.08	17.08
2	2.15	0.24	241.83	17.7	2.66	0.48	244.01	21.21

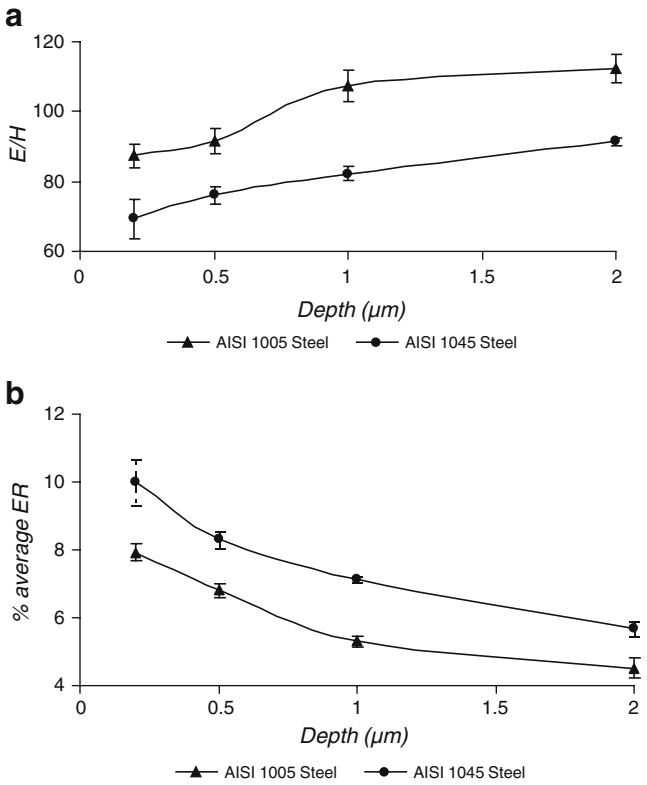

Fig. 2 Comparison of elastic modulus/hardness ratio (**a**) and percentage elastic recovery for workpiece specimens (**b**)

2.3 Experimental details and cutting parameters

To study the deformation and machining performance, micro-milling tests were under taken. The cutting tools used were flat end mills (Fraisa M5712080) with a diameter of 800 μm. These were manufactured from fine grain tungsten carbide and coated with TiAlN. The cutting edges had a rake angle of 6° and a helix angle of 25°. A tool diameter of 800 μm was selected since this falls within the 1 to 999-μm size range common for micro-milling. Additionally, the higher end of the micro-scale tool diameter range was ideal in order to minimise the chance of tool edge breakage and hence focus on workpiece-related machinability aspects. Prior to the cutting tests, each micro-end mill was imaged using a scanning electron microscope (SEM) and the average radii of the cutting edges were estimated from the SEM and found to be in the range of 1 to 2 μ.

The work presented here contributes to a theme of sustainable manufacture where the idea is to investigate the potential for dry or near dry machining. Dry machining can bring environmental and health safety benefits. Environmental regulations are expected to tighten up with regards to the use of machining coolants and lubricants [33]. Moreover, coolant mists and coolant coated chips need appropriate disposal. For these reasons, micro-slotting tests were performed dry on a Mikron HSM 400 milling centre. The static radial runout of spindle–collet tool system was measured in the clamped state before each cutting trial. The radial runout was estimated from the runout gauge measurements to be 1.6 μm in average, with a standard deviation of 0.76 μm.

The cutting parameters used are shown in Table 2. The range of maximum undeformed chip thickness (i.e. feed per tooth in slotting) was selected to cover values either side of the tool edge radius. This enabled the study of both negative and positive effective rake angles. Micro-milled slots having a 20 mm length of cut were made at each feed rate. The condition of each tool was observed before machining and re-inspected at stages during the cutting tests. The cutting trials were repeated twice for each experimental run.

3 Micro-milling results and discussions

3.1 Surface roughness

The surface topography on the floor of the micro-milled slots, for both workpiece materials, was analysed using a Wyko NT11000 optical profiler (white light interferometer) and Hitachi S-3400 SEM. Surface roughness was measured in 12 different positions across the length of the slot. The Wyko NT1100 surface profiler uses vertical scanning interferometry mode at 2.5× magnification, full resolution and 1× scan speed. The area sampled by the Wyko was 2.429 by 1.848 mm, with a picture resolution of 736 by 480, which yielded 3.3 μ/pixel. The resolution in Z axis was 1 nm. The average surface roughness (as well as the scatter in the measured values) was plotted against the corresponding feed rate, as shown in Fig. 3. The data shows that the surface roughness is significantly lower than the grain size. This presents the possibility of grain polishing or facture as an integral part of the mechanics of micro-machining for both workpiece materials.

The overall relationship between the surface roughness and maximum undeformed chip thickness is nonlinear for both workpiece materials. For 0.02 μm/tooth undeformed chip thickness, a substantially high surface roughness and highest scatter was recorded for AISI 1045 steel compared to AISI 1005. This can be attributed to the differences in elastic recovery of ferrite and pearlite as evident by the

Table 2 Process parameters

Spindle speed (rpm)	30,000
Chip load (μm/tooth)	0.02, 0.2, 0.5, 1, 2, 5, 10, 15
Axial depth of cut (μm)	75
Tool diameter (μm)	800

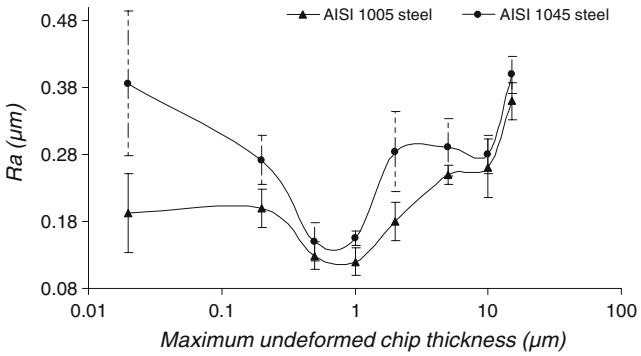

Fig. 3 Surface roughness

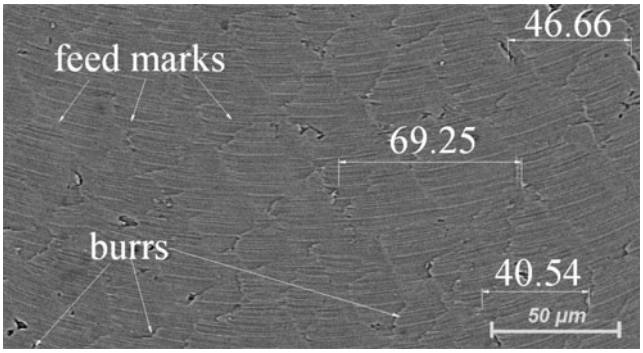

Fig. 5 Magnified area of AISI 1045 slot floor machined at 2 μm/tooth

higher elastic recovery for AISI 1045 in Fig. 2. The result suggests that micro-machining of a single phase material minimises the differential elastic recovery that would be found in multi-phase materials and hence improves surface finish.

In multiphase material, the value of minimum chip thickness is lower for a harder phase than a softer phase [12]. This variation in minimum chip thickness causes transition in cutting from one phase to another, affecting surface finish of machined parts. In this respect, the AISI

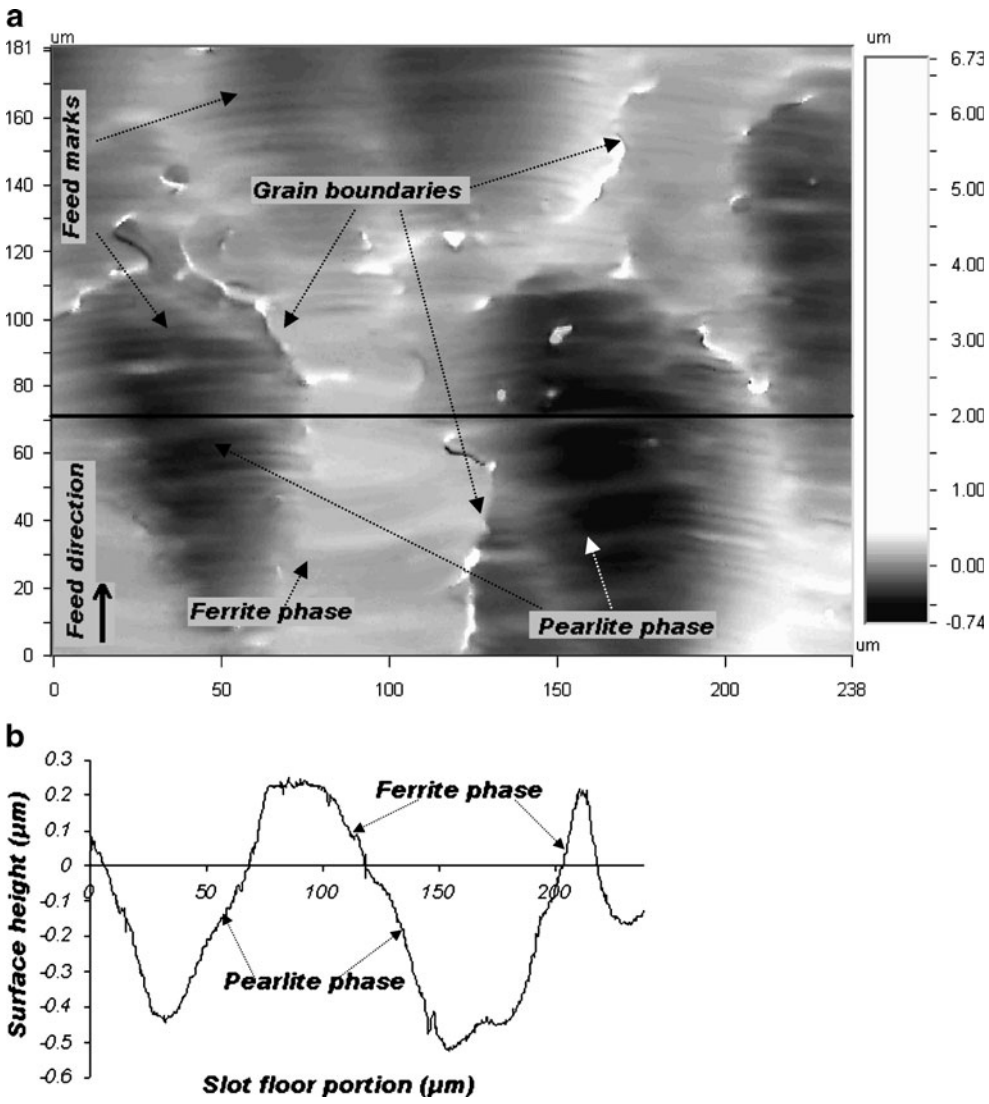

Fig. 4 Micro-milled slot base for AISI 1045 steel generated at 0.02 μm/tooth

1045 steel surface topography was examined after machining at 0.02 μm/tooth undeformed chip thickness (about 3% of edge radius). Figure 4a shows the image measured from Wyko optical profiler with a 0.32 μ/pixel resolution. Figure 4b is the 2D surface profile corresponding to a horizontal black line marked in the Fig. 4a. First, the dark and light regions correlate well with the average intercept length of the pearlite and ferrite phases. These were identified from Fig. 4a, and then the extracted surface profile for Fig. 4b was analysed across those areas. It shows concave and convex forms (differential elastic recovery) on the pearlite and ferrite grains respectively with cutting discontinuity across grain boundaries. This analysis was repeatable at different positions of the machined surface.

When machining at an undeformed chip thickness much smaller than the tool edge radius, the effective rake angle becomes highly negative and material spring-back effects

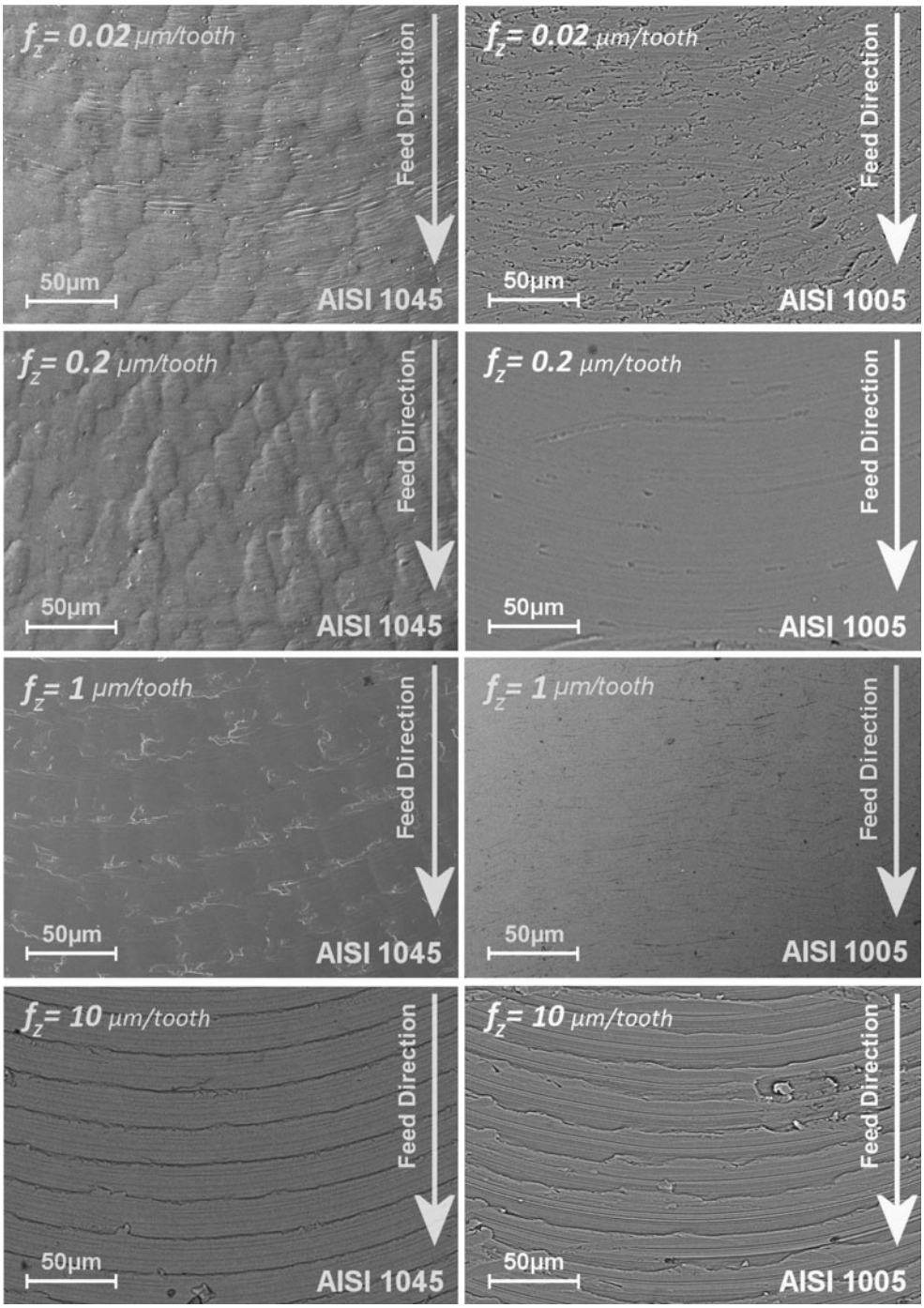

Fig. 6 Surface generated at different feed rates

need to be considered. In Fig. 3, as undeformed chip thickness is increased and approaches the tool edge radius, the rake angle becomes less negative, and the increase in surface roughness due to material spring-back effect is reduced. The best surface finish was achieved at feed per tooth of 1.0 μm/tooth for both workpiece materials. This feed per tooth is comparable to the tool edge radius and located at the lower end of the tool edge radius values for the tools used. This suggests that in the process planning for these workpiece materials, knowledge of the tool edge radius is important.

Again in Fig. 3, as the feed per tooth increases beyond the tool edge radius, the difference in surface roughness value between the two materials appears more pronounced at 2 μm/tooth undeformed chip thickness. It is noted that at 2 μm/tooth undeformed chip thickness, this length scale is shorter than the average width of the ferrite phase. Thus, one possible explanation for surface roughness trends observed could be due to the discontinuity (see Fig. 5) in cutting process across the grain boundary and the formation of a comparatively thicker miniature burr on the grain boundary of AISI 1045 steel. Formation of grain boundary burrs was also reported by Volger et al. [12]. Moreover, Fig. 3 shows that the surface roughness does not significantly increase as the feed rate is increased from 2 to 10 μ as expected. A possible explanation is that at the lower feed rate (2 μ) the formation of burrs at the grain boundaries is more pronounced than at higher feed rates. This has the effect of masking the traditional increase in surface roughness expected when using higher feed rates. However, at higher feed rates, the conventional trend of increasing roughness with increasing feed rate as encountered in macro-scale machining also holds for micro-cutting for the signal phase ferritic steel.

The surface generated was studied at feeds per tooth below minimum chip thickness (0.02 μm/tooth), within the vicinity of the minimum chip thickness (0.2 μm/tooth), comparable to (1 μm/tooth) and above the tool edge radius (10 μm/tooth). These cases are presented for both materials in Fig. 6. The minimum chip thickness has been reported in literature for various workpiece materials [12, 34, 35]. Generally, images for AISI 1005 steel clearly show smoother surface appearance compared to AISI 1045 steel. However, AISI 1005 steel shows a smeared

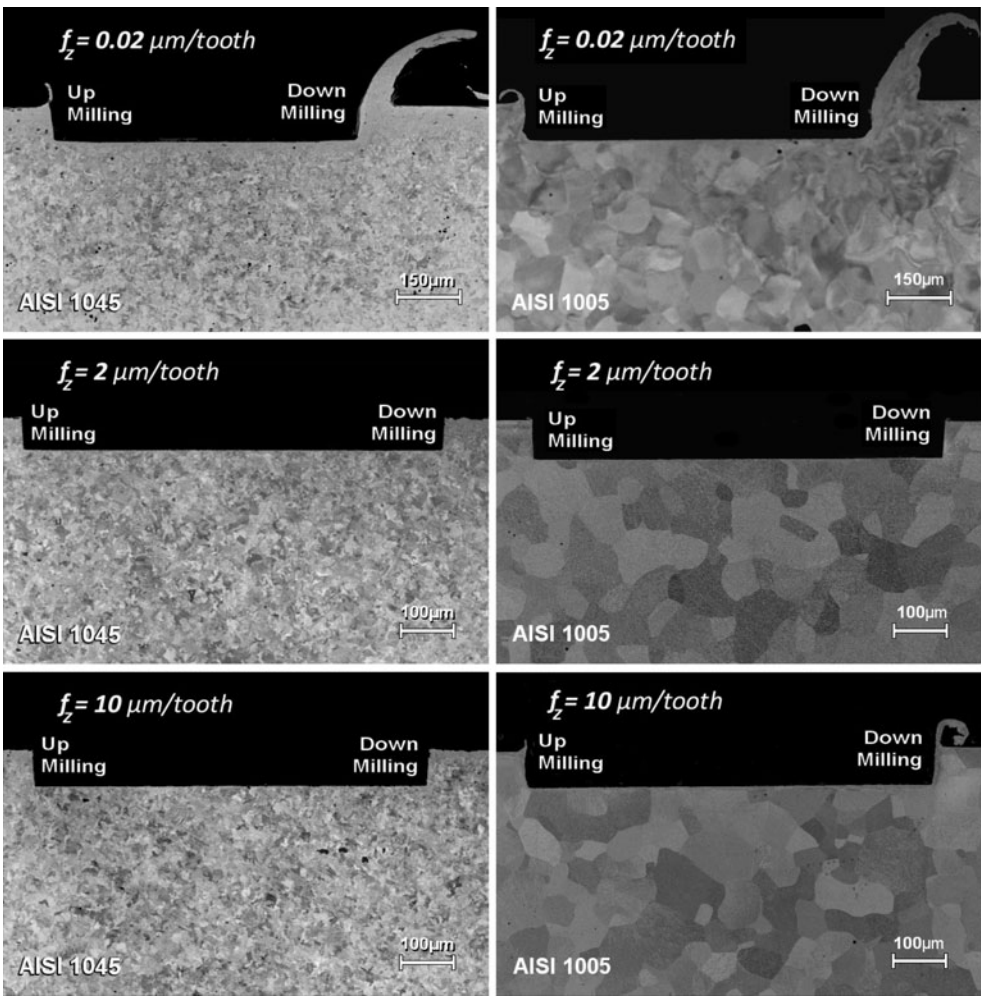

Fig. 7 Subsurface microstructural modification and material side flow

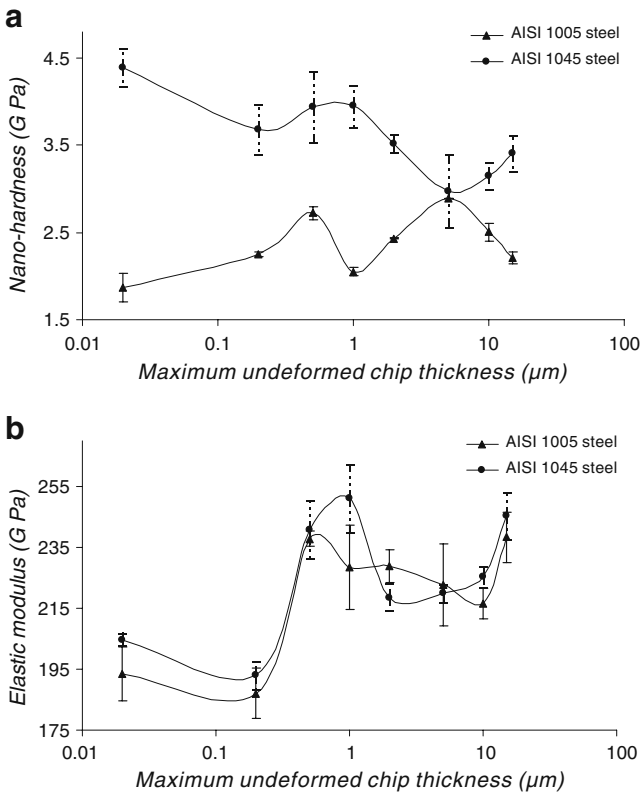

Fig. 8 Slot floor subsurface layer properties. **a** Nano-hardness. **b** Elastic modulus

pattern which could be attributable to higher plastic deformation at 0.02 μm/tooth. At a feed per tooth of 0.2 μm, material microstructure effects dominate the surface texture of AISI 1045 workpiece material. Additionally, burr formation can be observed on the image of AISI 1045 steel machined at 1 μm/tooth undeformed chip thickness. Above the tool edge radius, feed marks dominate the surface form.

3.2 Subsurface microstructure modification

To investigate subsurface deformation and microstructure change, each slot was sectioned and then set in a conductive acrylic hot resin in order to reduce edge rounding during polishing. Scanning electron microscopy and nano-hardness testing was performed at the two sides and centre of the slots. Figure 7 shows the material side flow and grain structure for micro-machined slots. In AISI 1005 steel, at lowest feed rate, the thickness of material being pushed out (extruded) to form a burr is of comparable magnitude to the grain size of the material. For all cases tested, AISI 1045 steel demonstrated better edge definition geometry than AISI 1005. Thus, AISI 1005 with a lower hardness and higher plastic deformation (as discussed before) generates larger burrs compared to AISI 1045.

To characterise the machined surface, nano-indentation was performed. An indentation depth of 0.5 μm was selected and a series of tests were carried out at a minimum distance (~10 μm) from the edge of the slot to avoid lateral push away of the material. These results are based on repeating measurements with identical process parameters on both workpiece materials. The tests were performed on sectioned pieces taken before the end of second slots. Further measurements revealed similar trends; therefore the results can be seen as quantitatively significant. The nano-hardness and elastic modulus of the modified surface layer at the centre of the slot is shown in Fig. 8. Each dot on the graph represents the average value and the bars represent the standard error of the mechanical properties measured from five points on the slot floor. Figure 8a shows that AISI 1045 steel exhibit work hardening during the chip formation process when compared to AISI 1005 steel. The AISI 1045 steel produces harder surface than bulk material in the ploughing zone, while micro-machining of AISI 1005 steel induces no noticeable change in hardness for most investigated feed per tooth. The former can be attributable to higher wear land (will be discussed in Section 3.4) which contributed to higher tertiary zone temperatures and hence promoting surface modification. It is also worth mentioning here that elastic modulus substantially decreases for both workpieces at the feed rates less than 20% of the tool edge radius (Fig. 8b).

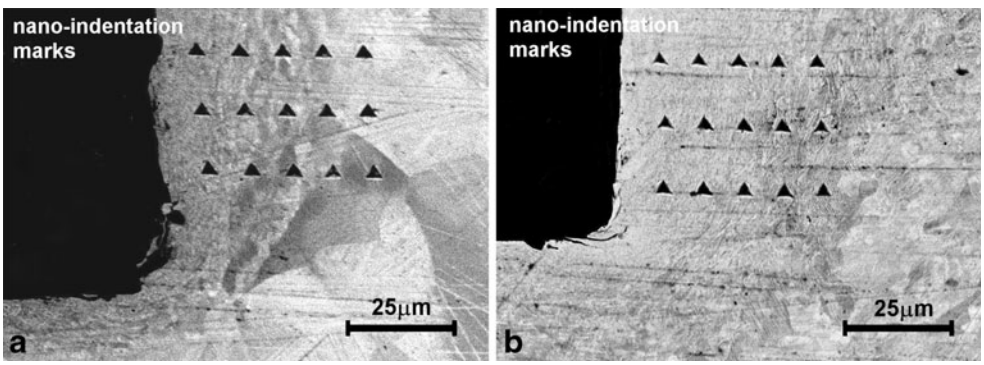

Fig. 9 Slot down-milled side. **a** AISI 1005. **b** AISI 1045

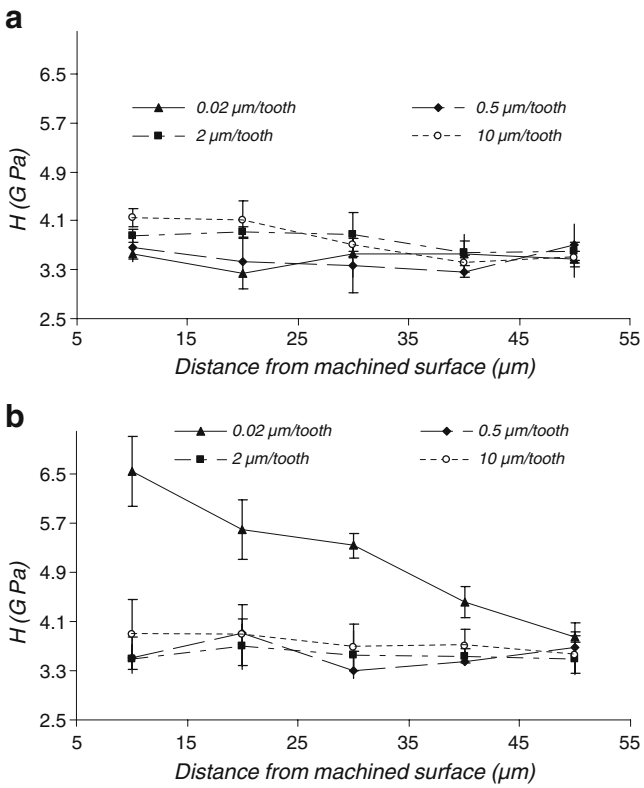

Fig. 10 AISI 1045 steel nano-hardness in-depth profiles generated at up-mill side wall (**a**) and down-mill side wall (**b**)

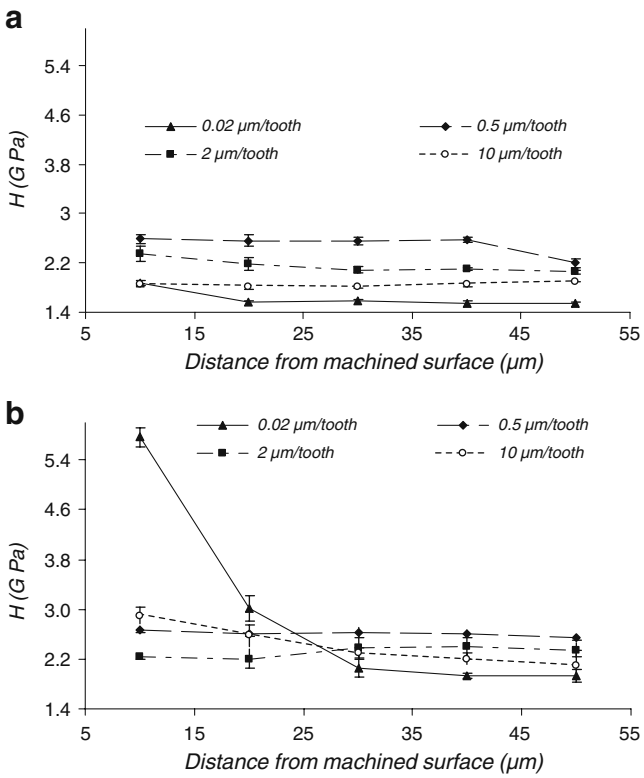

Fig. 11 AISI 1005 steel nano-hardness in-depth profiles generated at up-mill side wall (**a**) and down-mill side wall (**b**)

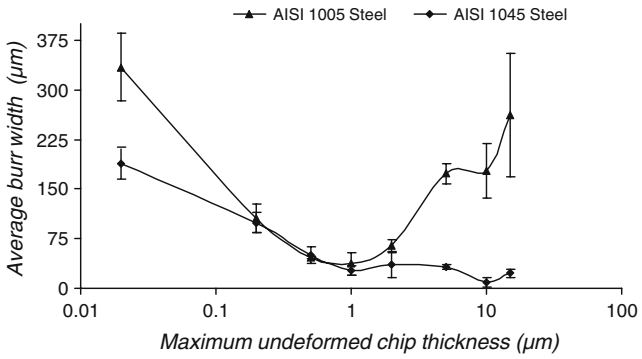

Fig. 12 Burr size in down-milling

Figure 9 shows the nano-indentation marks on the down milling side of the slot for both workpiece materials machined at 0.02 μm/tooth. The depth below the wall surface for the initial point of indentation was specified by positioning the indenter approximately 10 μm below the wall surface. The indentations then followed an automated process until 15 nano-indentations had been carried out in the form of 3×5 arrays for both sides. The indents were 10 μm apart from each other; this provided three indents placed parallel at the same distance from the respective wall surface. After performing the array of indents, back-scattered electrons (BSE) images were taken in the indented area to ensure the position of indents for all cases.

Figures 10 and 11 show in-depth nano-hardness profiles across up-milled and down-milled sides of the slot machined at four different feed rates on AISI 1045 and AISI 1005 steel, respectively. The most noticeable increase in hardness was recorded in the subsurface region at the down milling side of the slot wall at the lowest undeformed chip thickness for the both workpiece materials. The results demonstrate that mode of milling imparts differential change in the properties of machined surfaces. When machining below the critical undeformed chip thickness, applying the 0.37 and 0.32 standard deviation from Table 1 to the results after machining in Figs. 10 and 11 does not mask the distinct trends for the two workpiece materials.

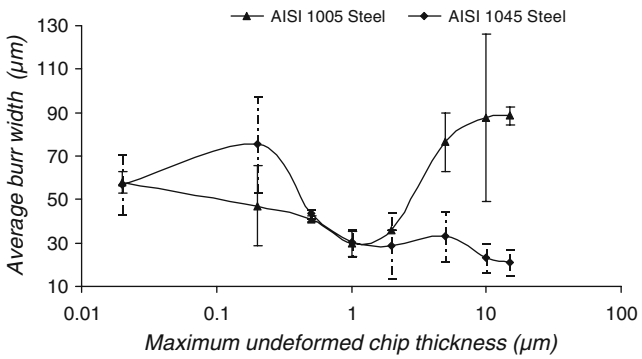

Fig. 13 Burr size in up-milling

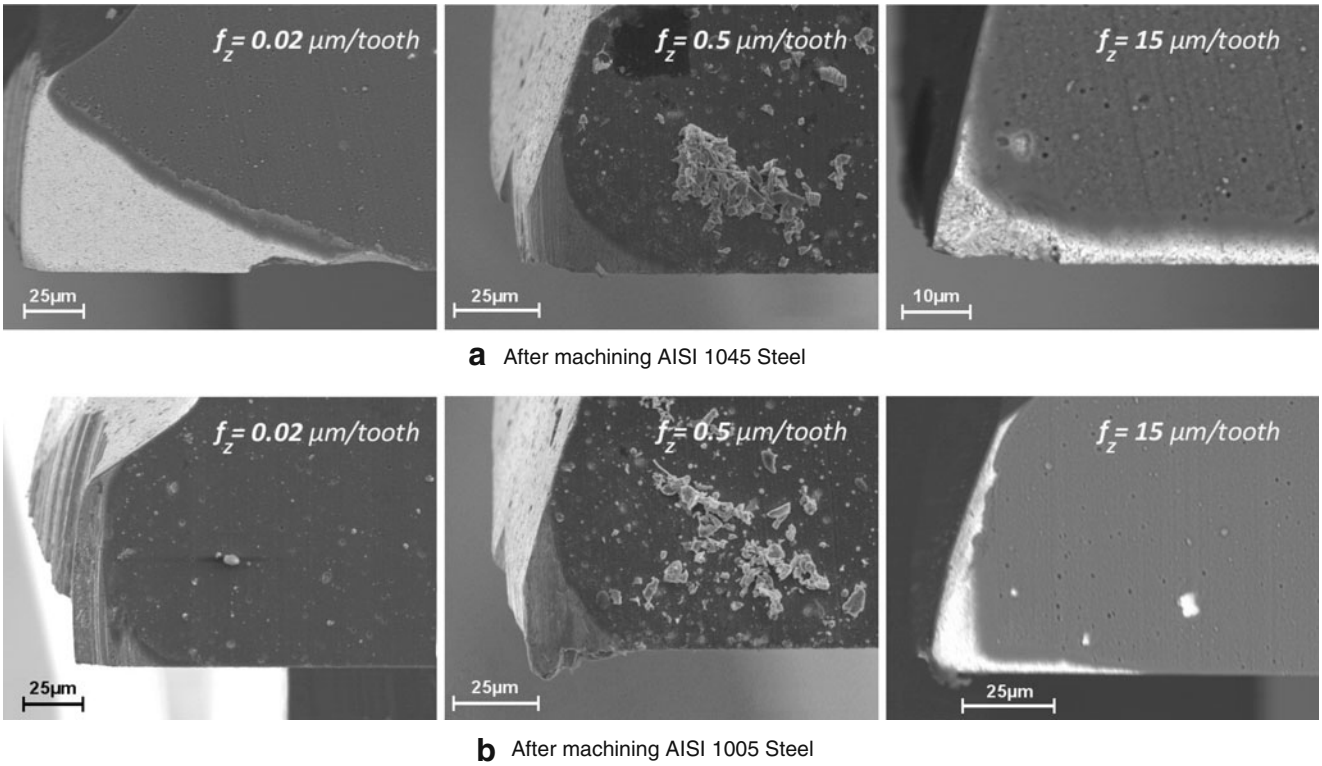

Fig. 14 Material deformation effects on the tool cutting edges

Moreover, it is clear from Fig. 9 that the depth of deformed zone can be in the order of 40 µ. These results imply that the micro-machining process modifies the properties of the workpiece material in regions of plastic deformations.

At lowest undeformed chip thickness, the value of nano-hardness correlates well with the flank wear. The results suggests that a sharp tool (without or with small wear) induced no appreciable change in nano-hardness. While a worn tool results in surface modification and increase in hardness.

3.3 Burr formation

There is no common approach in terms of measuring curled 3D burr shape, especially in the micro domain. What emerges from the past literature is that the burr shapes can be qualitatively compared according to the shape [26, 27] or quantitatively measured in terms of burr width [36, 37] and burr height [38]. Both burr height and width do not reflect the fact that the burr could be curled. However, in terms of component functionality, use and assembly of burr height and width are relevant measures. In the available techniques, measurement of burr width was chosen to quantify the burrs formed at the top of the slot since this is a parameter that could be more accurately measured by the Wyko. Focussing the microscope on the apparent top of the burr is difficult with the optical instrument.

The top burr width in both up and down milling was measured from Wyko scans. The variation of the burr width as a function of maximum undeformed chip thickness is shown in Figs. 12 and 13 for the both workpiece materials. The error bars of the figures were obtained using the standard error calculated from 15 measurements. Over the entire range of feed rates investigated, AISI 1005 steel produced larger burr on the down milling side compared to AISI 1045 steel. This can be attributable to the higher ductility of AISI 1005. It was noted that when the feed per tooth was lower than the tool edge radius, the tool wear (discussed later in Section 3.4) considerably leads to increased top burr size especially on the down milling side. Interestingly for the up milling side, the effect of tool wear

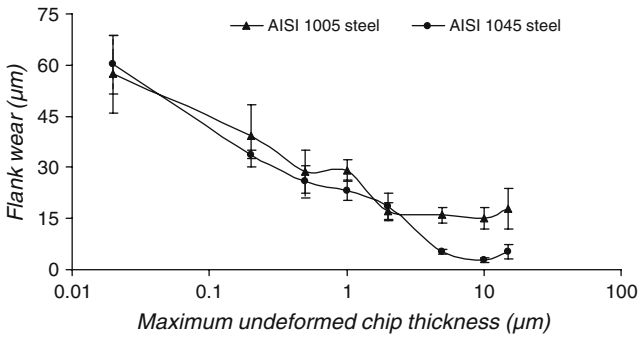

Fig. 15 Flank wear comparison

on burr generation is less dominant at these feed rates. The differences in the burr size between the two milling modes may be due to the burr formation mechanisms and vibration.

3.4 Tool wear

Again in the brief literature review, no unified approach for tracking the condition of micro tools is available. The change in tool diameter [26], edge radius roundness [39] and flank wear measurement from the bottom view of the end mills [36] were the criteria that researches have identified for the evaluation of tool wear in micro domain. Moreover, for steels, it was evident that trends for flank wear at the bottom cutting edge, edge chipping, cutting edge radius enlargement and percentage tool diameter reduction are positively correlated [40]. It is therefore reasonable to monitor any one of these parameters to assess tool performance in terms of tool life. The tool bottom face is directly in contact with slot floor surface, affecting the surface finish. Therefore, this parameter was adopted in this research.

In contrast to the flat end mills used here, ball nose micro-cutters could be considered to increase the cutting edge strength. However, it was noted that in developing technology for ultimately machining inclined slots, ball nose micro tools suffer from push off and deflection and this affects tool life. Thus, this study was based on the flat end mills.

Tool wear progression was observed by taking SEM images before and after machining. Some images of the used cutting edges are shown in Fig. 14, corresponding to a material removal of 1.2 mm^3. It is clear from these images that cutting tools used for machining AISI 1045 experienced more uniform and abrasive wear while those used for machining AISI 1005 have flank faces characterised by plastic deformation.

Figure 15 shows a comparison of maximum flank wear land measured on both flutes from the bottom view of the micro-end mill after completion of slots. A relatively higher degree of flank wear was observed when machining the softer AISI 1005 material in line with the higher plastic deformation. For both workpiece materials, the reduction in the flank wear as the feed rate increased is consistent with reduced ploughing effects.

4 Conclusions

The work presented in this paper compared material phase effects, in micro-milling over a range of undeformed chip thickness spanning the tool edge radius and grain sizes of two selected workpiece materials. For this range, surface finish, microstructure change, burr formation and tool wear were investigated for the two kinds of steel. Some of the significant findings from this study can be summarised as follows:

- The results show that in terms of surface finish, the machinability of AISI 1045 compared to AISI 1005 steel is more challenging due to cutting discontinuities and formation of grain boundary burrs.
- The challenge in machining AISI 1005 relates to edge profile definition as driven by burr size growth.
- The best surface finish was obtained at feed rates closer to the tool edge radius for both workpiece materials. This suggests that generation of the best surface finish was more sensitive to tool edge radius than material grain size.
- AISI 1045 steel which was predicted to exhibit a higher elastic recovery also had a higher surface roughness compared to AISI 1005. Thus, it is possible that in AISI 1045 alloy steel, differential elastic recovery between the phases compromises surface finish.
- For AISI 1005 alloy steel, higher plastic deformation as predicted by nano-indentation tests promotes relatively larger burrs in the down milling mode compared to micro-machining of AISI 1045 steel.
- At undeformed chip thickness lower than the tool edge radius, burr size increases with reduced feed rates.
- The micro-milling process increases the nano-hardness of the workpiece material in the down milling mode. This property modification as driven by milling mode is differential on milled surface profiles.
- The results suggest that nano-indentation measurements can be used to provide a qualitative relative assessment of micro-machinability for different workpiece materials and hence, reduce the cost and time of technology development.

Acknowledgements The authors acknowledge the support offered by Engineering and Physical Sciences Research Council (EPSRC) under grant DT/E010512/1 and the supply of Materials by Corus.

References

1. Bissacco G, Hansen HN, De Chiffre L (2005) Micromilling of hardened tool steel for mould making applications. J Mater Process Technol 167(2–3):201–207
2. Chae J, Park SS, Freiheit T (2006) Investigation of micro-cutting operations. Inter J Mach Tools and Manuf 46(3–4):313–332
3. Dornfeld D, Min S, Takeuchi Y (2006) Recent advances in mechanical micromachining. Ann CIRP 55(2):745–768
4. Schmidt J, Tritschler H (2004) Micro cutting of steel. Microsystem Technologies 10(3):167–174
5. Weule H, Huntrup V, Tritschler H (2001) Micro-cutting of steel to meet new requirements in miniaturization. Ann CIRP 50(1):61–64

6. Simoneau A, Ng E, Elbestawi MA (2006) Chip formation during microscale cutting of a medium carbon steel. Inter J Mach Tools and Manuf 46(5):467–481
7. Simoneau A, Ng E, Elbestawi MA (2006) The effect of microstructure on chip formation and surface defects in microscale, mesoscale, and macroscale cutting of steel. Ann CIRP 55 (1):97–102
8. Moronuki N, Liang Y, Furukawa Y (1994) Experiments on the effect of material properties on microcutting processes. Precision Eng 16(2):124–131
9. Zhou M, Ngoi BKA, Zhong ZW, Wang XJ (2001) The effect of material microstructure on microcutting processes. Mater Manuf Processes 16(6):815–828
10. Mian AJ, Driver N, Mativenga PT (2009) Micromachining of coarse-grained multi-phase material. P I Mech Eng B-J Eng Manuf 223(4):377–385
11. Bissacco G, Hansen HN, De Chiffre L (2006) Size effects on surface generation in micro milling of hardened tool steel. Ann CIRP 55(1):593–596
12. Vogler MP, DeVor RE, Kapoor SG (2004) On the modeling and analysis of machining performance in micro-endmilling, Part I: surface generation. J Manuf Sci Eng, Trans ASME 126(4):685–694
13. Zhou M, Ngoi BKA (2001) Effect of tool and workpiece anisotropy on microcutting processes. P I Mech Eng B-J Eng Manuf 215(1):13–19
14. Simoneau A, Ng E, Elbestaw MA (2007) Grain size and orientation effects when microcutting AISI 1045 steel. Ann CIRP 56(1):57–60
15. Simoneau A, Ng E, Elbestawi MA (2006) Surface defects during microcutting. Inter J Mach Tools and Manuf 46(12–13):1378–1387
16. Son SM, Lim HS, Ahn JH (2005) Effects of the friction coefficient on the minimum cutting thickness in micro cutting. Inter J Mach Tools and Manuf 45(4–5):529–535
17. Li H, Lai X, Li C, Feng J, Ni J (2008) Modelling and experimental analysis of the effects of tool wear, minimum chip thickness and micro tool geometry on the surface roughness in micro-end-milling. J Micromechanics Microeng 18(2):1–12
18. Furukawa Y, Moronuki N (1988) Effect of material properties on ultra precise cutting processes. Ann CIRP 37(1):113–116
19. Popov K, Dimov S, Pham DT, Minev R, Rosochwski A (2006) Micro milling: material microstructure effects. P I Mech Eng B-J Eng Manuf 220(11):1807–1813
20. Takács M, Verö B, Mészáros I (2003) Micromilling of metallic materials. J Mater Process Technol 138(1–3):152–155
21. Gillespie LK (1979) Deburring precision miniature parts. Precision Eng 1(4):189–198
22. Gillespie LK, Blotter PT (1976) The formation and properties of machining burrs. J Manuf Sci Eng, Trans ASME 98:66–74
23. Hashimura M, Chang YP, Dornfeld DA (1999) Analysis of burr formation mechanism in orthogonal cutting. J Manuf Sci Eng, Trans ASME 121(1):1–7
24. Nakayama K, Arai M (1987) Burr formation in metal cutting. Ann CIRP 36(1):33–36
25. Schaller T, Bohn L, Mayer J, Schubert K (1999) Microstructure grooves with a width of less than 50 μm cut with ground hard metal micro end mills. Precision Eng 23(4):229–235
26. Filiz S, Conley CM, Wasserman MB, Ozdoganlar OB (2007) An experimental investigation of micro-machinability of copper 101 using tungsten carbide micro-endmills. Inter J Mach Tools and Manuf 47(7–8):1088–1100
27. Lee K, Dornfeld DA (2002) An experimental study on burr formation in micro milling aluminium and copper. Transactions of the NAMRI/SME 30:255–262
28. Fang FZ, Liu YC (2004) On minimum exit-burr in micro cutting. J Micromechanics Microeng 14:984–988
29. British Standard: Steels—micrographic determination of the apparent grain size, BS EN ISO 643:2003
30. Gouldstone A, Chollacoop N, Dao M, Li J, Minor AM, Shen YL (2007) Indentation across size scales and disciplines: recent developments in experimentation and modeling. Acta Mater 55(12):4015–4039
31. Jardret V, Zahouani H, Loubet JL, Mathia TG (1998) Understanding and quantification of elastic and plastic deformation during a scratch test. Wear 218(1):8–14
32. Nakayama K (1997) Topics on fundamentals of precision machining. Machining Sci Technol 1(2):251–262
33. Aronson RB (1995) Why dry machining? Manuf Eng 114(1):33–36
34. Basuray PK, Misra BK, Lal GK (1977) Transition from ploughing to cutting during machining with blunt tools. Wear 43:341–349
35. Liu X, DeVor RE, Kapoor SG (2006) An analytical model for the prediction of minimum chip thickness in micromachining. J Manuf Sci Eng, Trans ASME 128(2):474–481
36. Aramcharoen A, Mativenga PT, Yang S, Cooke KE, Teer DG (2008) Evaluation and selection of hard coatings for micro milling of hardened tool steel. Inter J Mach Tools and Manuf 48(14):1578–1584
37. Aramcharoen A, Mativenga PT (2009) Size effect and tool geometry in micromilling of tool steel. Precision Eng 33(4):402–407
38. Park JB, Wie KH, Park JS, Ahn SH (2009) Evaluation of machinability in the micro end milling of printed circuit boards. P I Mech Eng B-J Eng Manuf 223(11):1465–1474
39. Lee K, Dornfeld DA (2005) Micro-burr formation and minimization through process control. Precision Eng 29(2):246–252
40. Aramcharoen A, Mativenga PT (2008) Tool wear modes in micro/mesoscale milling of hardened die steel. CIRP 3rd International conference high performance cutting (HPC), vol. 1. Dublin, Ireland, pp 179–188